

Inertial Stability and Phase Error of Time Integration Schemes in Ocean General Circulation Models

JIA WANG

Ocean Prediction Experimental Laboratory and Division of Applied Marine Physics, Rosenstiel School of Marine and Atmospheric Science, University of Miami, Miami, Florida

MOTO IKEDA

Graduate School of Environmental Earth Science, Hokkaido University, Sapporo, Japan

(Manuscript received 11 July 1996, in final form 11 November 1996)

ABSTRACT

Numerical finite-difference schemes of time integration in widely used ocean general circulation models are systematically examined to ensure the correct and accurate discretization of the Coriolis terms. Two groups of numerical schemes are categorized. One group is suitable for simulating an inertial wave system and geostrophic adjustment processes in the ocean with the necessary condition for stability being $|F| = |f| \Delta t < 1$ (where f is the Coriolis parameter and Δt is the integration time step in the model), such as the predictor–corrector scheme (as shown in this study), the most commonly used leapfrog scheme (as used in MICOM, POM, SPEM, and many others), Euler-centered scheme (as used in SOMS), and leapfrog scheme plus Euler-centered Coriolis terms [as used in the Geophysical Fluid Dynamics Laboratory (GFDL) model]. The other group is able to serve as a long-term climate study using a large integration time step that may violate $|F| = |f| \Delta t < 1$ by damping out inertial waves, such as the GFDL scheme plus Euler-backward Coriolis terms and the Euler predictor–corrector scheme plus an implicit treatment of the Coriolis terms used in OPYC model. Caution is made regarding the use of the Euler-forward and other schemes that produce unstable inertial waves; this problem could be serious for a calculation longer than one week. The predictor–corrector scheme is recommended as a replacement for the simple Euler-forward scheme. The explicit leapfrog and predictor–corrector schemes tend to overestimate the phase frequency, whereas the Euler schemes and implicit schemes underestimate it. To better simulate the correct phase frequency, $F < 0.1$ is recommended. Furthermore, an alternate use of an explicit scheme (e.g., leapfrog) and an implicit scheme (e.g., Euler backward or Masuno scheme, etc.) is strongly recommended to preserve the correct phase frequency.

1. Introduction

The inertial oscillation is a ubiquitous feature in the ocean. It generally produces anticyclonic oscillatory ocean currents (Pollard and Millard 1970; Tee 1979; Maas and Haren 1987) in both hemispheres. In studies of Ekman dynamics due to wind forcing (Maas and Haren 1987), intertidal currents, interactions among wind-induced storms, tides and inertial oscillations, and geostrophic adjustment in the ocean and coastal seas, inertial motion plays an important role.

There have been many observational studies that indicate this common phenomenon of inertial oscillations in the ocean. The spatial structure of inertial-period motions in the North Sea was observed by Schott (1970)

and Maas and Haren (1987). Millot and Crepon (1981) also observed inertial oscillations on the continental shelf of the Gulf of Lion (northwestern Mediterranean Sea). Interestingly, near-inertial waves with horizontal scales of about 10 km were observed in the North Pacific subtropical front by Kunze and Sanford (1984). Wang et al. (1991) also found strong inertial oscillations in baroclinic currents in an observational study of internal tides in the Laurentian Channel, Canada; rotating Poincaré waves and inertial currents were also detected.

In primitive equation ocean general circulation models, the inertial mode naturally exists if the Coriolis terms are explicitly included. The Coriolis force not only produces a rotating wave and current system, but also introduces a numerical stability constraint (the “inertial constraint”) in the finite-difference equations (Wang 1996). However, if the finite-difference scheme for the Coriolis terms is not correctly and accurately discretized, the numerical (artificial) inertial instability in the model will ruin the physical processes. This is the difference between geophysical fluid dynamics and ordi-

Corresponding author address: Dr. Jia Wang, Ocean Pollution Research Center, Rosenstiel School of Marine and Atmospheric Science, University of Miami, 4600 Rickenbacker Causeway, Miami, FL 33149.
E-mail: jia.wang@rsmas.miami.edu

TABLE 1. The names of the most commonly used ocean general circulation models (OGCMs), their time difference schemes, and the manners of discretizing the Coriolis terms.

Name of OGCM	References	Time-difference scheme/the Coriolis term, C
ECOMSI	Blumberg (1991)	Euler forward/ C^n
SOMS	Dietrich et al. (1987)	Euler forward/ $[(1 - \beta)C^n + \beta C^{n+1}]$ ($\beta = 0.5$)
OPYC	Oberhuber (1993)	Euler forward predictor-corrector/ $[(1 - \beta)C^n + \beta C^{n+1}]$ ($0.5 \leq \beta \leq 1$)
MICOM	Bleck et al. (1992)	Leapfrog/ C^n
POM	Mellor (1991)	
SPEM	Haidvogel et al. (1991)	
GFDL (or MOM)	Bryan (1969), Cox (1984)	Leapfrog/ $[(1 - \beta)C^n + \beta C^{n+1}]$ ($0 \leq \beta \leq 1$; usually set $0.5 \leq \beta \leq 1$; note that β is α in the GFDL model)

nary fluid mechanics with no Coriolis force. The question arises as to how well a finite-difference scheme captures the real physics of this phenomenon (or reproduces the solution of the corresponding differential equation) in the ocean.

Many efforts have been made to successfully control nonlinear instability in numerical models even though the advection terms are usually small or one order of magnitude smaller than the other terms in the governing equations. In addition to the fact that the nonlinear terms must be correctly discretized to conserve energy and mass in the finite-difference equations of a model, more attention should be paid to the dominant terms in the dynamic equations of interest. In large-scale ocean dynamics, for instance, the geostrophic balance is the first-order approximation in which the pressure gradient and Coriolis terms are comparable and dominant. In coastal, small-scale, tidal dynamics, the inertia-gravity waves, the rotating Poincaré waves, and inertial oscillations are the major physical processes in which the pressure gradient, Coriolis, time derivative, and dissipation terms are dominant. Thus, in any numerical model, these four terms (pressure gradient, Coriolis, time derivative, and dissipation terms) must be correctly and precisely discretized to maintain the physics in the original continuum medium. The purpose of this study is to address which finite-difference scheme is correctly and accurately formulated to best simulate the inertial oscillations. If researchers are going to use an existing model as a tool to study and to simulate these processes, which model or scheme should they choose: the Geophysical Fluid Dynamics Laboratory [GFDL or MOM (which stands for molecular ocean model)] model (Bryan 1969; Cox 1984), the Princeton Ocean Model (POM, Mellor 1991), ECOMSI (Blumberg 1991), SOMS (Dietrich et al. 1987), MICOM (Bleck et al. 1992), SPEM (Haidvogel et al. 1991), or OPYC model (Oberhuber 1993)?

Grotjahn and O'Brien (1976) examined some inaccuracies in finite-difference hyperbolic equations, including inertial oscillations. They focused on the general truncation or round-off error caused by the discretization of the differential equations into finite-difference equations. Mesinger and Arakawa (1976) and O'Brien (1986) examined some commonly used time-integration schemes for a nondissipative system. However, they did

not examine phase-frequency errors. Becker and Deleersnijder (1993) examined stability of an inertia-gravity wave system with no dissipation; the phase-frequency errors were not examined either. Dukowicz and Smith (1994) systematically investigated stability of an inertia-gravity-Rossby wave system with no dissipation in the implicit, free-surface Bryan-Cox-Semtner ocean model. The phase change of each mode was also examined in comparison to the analytical solution. Wang (1996), for the first time, proposed the concept of the "global stability" and examined the linear global stability of the 2D shallow-water dynamic and thermodynamic system (an inertia-gravity wave system) with advection and dissipation. A series of global stability criteria were derived, including the inertial constraint $|F| = |f| \Delta t < 1$, in the leapfrog and centered difference equations. Again, no phase-frequency error information was provided.

In this study, we emphasize both stability and phase-frequency error of different time integration schemes (rather than space) for a pure, dissipative, inertial wave system and compare the amplification factor and phase frequency of each scheme to the analytical solutions. The purpose is to compare advantages and disadvantages of these schemes that have been employed in the following models (see Table 1): 1) the GFDL model (leapfrog scheme plus an implicit approach to the Coriolis terms); 2) the MICOM, POM, SPEM, and many others (leapfrog scheme plus an explicit centered differencing for the Coriolis terms); 3) the SOMS (Euler-forward scheme in time plus the Euler-centered Coriolis terms); and 4) the OPYC model (Euler-forward predictor-corrector scheme plus an implicit approach to the Coriolis terms). We also examine other schemes, such as the two-time-step explicit Euler-forward scheme (Blumberg 1991) and predictor-corrector scheme developed in this study to replace the unstable Euler forward scheme.

In section 2, we start by obtaining the exact solution to inertial oscillations in the ocean, set up different numerical schemes, and perform stability and phase-frequency error analyses of each scheme. In section 3, we compare the numerical solutions from the different schemes to the analytical exact solutions to quantify each scheme. Finally, we summarize our findings in section 4.

2. Stability and phase frequency of time integration schemes

a. Governing equations and analytical solution

To focus on integration time schemes and discretization of the Coriolis terms, we choose the simple, linear momentum equations for a one-layer system without any horizontal variability. The rigid-lid approximation is applied, as in the GFDL model (Cox 1984) and SOMS (Dietrich et al. 1987). The equations contain the Rayleigh friction terms as well. The reason for choosing this simple system is that an analytical solution can be obtained as seen below:

$$\frac{\partial u}{\partial t} - fv = -ru, \quad \frac{\partial v}{\partial t} + fu = -rv \quad (1)$$

or

$$\frac{\partial w}{\partial t} + (if + r)w = 0 \quad (2)$$

in a complex form, where u , v , t , f , and r are horizontal velocities in x and y directions; time; the Coriolis parameter [$=2\Omega \sin(\phi)$, where $\Omega = 7.292 \times 10^{-5} \text{ s}^{-1}$ and ϕ is the latitude]; and the linear bottom friction coefficient (s^{-1}), respectively. The term $w = u + iv$ is the complex velocity with $i = (-1)^{1/2}$. The solutions to u and v subject to the initial conditions: $u_0 = 1$ and $v_0 = 0$ ($w_0 = 1$) are

$$(u, v) = e^{-rt}[\cos(ft), -\sin(ft)] \quad (3)$$

or

$$w = e^{-rt + i\omega_E t} \quad (4)$$

in a complex form, where $\omega_E = -f$ is the exact frequency of the inertial wave. The analytical inertial oscillations (with amplitude of unity if $r = 0$) will be compared with the numerical results using finite-difference schemes in both nondissipative ($r = 0$) and dissipative ($r \neq 0$) cases. With $r = 0$, Mesinger and Arakawa (1976) and O'Brien (1986) examined only the stability of some of the schemes included in this study, while they did not discuss phase-frequency error. It is very important to understand the features of the phase-frequency error for each case in order to remove the error by alternating among them. For instance, a leapfrog scheme that speeds up the phase frequency and the Matsuno (or Euler backward) scheme (Mesinger and Arakawa 1976) that slows down the phase frequency are alternated for the time integration in the GFDL model.

b. Euler-forward, Euler-centered, and Euler-backward (implicit) schemes

In some numerical models, Eq. (2) is differenced using the following two-time-step scheme:

$$w^{n+1} = (1 - R)w^n - iF [\beta w^{n+1} + (1 - \beta)w^n], \quad (5)$$

where $0 \leq \beta \leq 1$, $F = f\Delta t$, $R = r\Delta t$, and n and $n + 1$ denote the old and new time steps, respectively. Note that this scheme becomes a Euler-forward scheme if $\beta = 0$ (Blumberg 1991), Euler-centered scheme if $\beta = 0.5$ (Dietrich et al. 1987; Oberhuber 1993), and Euler-backward scheme if $0.5 < \beta \leq 1$ (Kwizak and Robert 1971; Robert et al. 1972; Oberhuber 1993), respectively. The model becomes nondissipative or contains free inertial motion when $r = 0$ (no dissipation).

To obtain the numerical stability criterion, we assume the solution having a Fourier wave form following Wang (1996):

$$w = De^{i\omega n \Delta t} = D\lambda^n, \quad (6)$$

where $\lambda = \exp(i\omega\Delta t)$, i , ω , Δt , and n are the eigenvalue, imaginary number, phase frequency, integration time step, and time at n , respectively. The term $D = U_0 + iV_0$ is the constant amplitude of the velocities. If $|\lambda| = 1$, <1 , or >1 , then the numerical solution is neutral, decaying, or growing (unstable) in amplitude. Thus, the stability problem becomes an estimate of the magnitude of the eigenvalue, λ . The phase frequency ω will be analytically derived as well.

Substituting (6) into (5) gives the solution as

$$\lambda = \frac{[(1 - R) - F^2\beta(1 - \beta)] - iF(1 - \beta R)}{1 + F^2\beta^2}. \quad (7)$$

We observe that if the Coriolis force, which introduces truncation error to the finite-difference equations, is neglected (i.e., $F = 0$), then the true solution to λ is $|\lambda| = 1 - R$ for $r \neq 0$ and unity for $r = 0$.

If $\beta = 0$, the scheme becomes the Euler-forward scheme. Taking the absolute value or modulus of (7) gives

$$|\lambda| = \begin{cases} (1 + F^2)^{1/2} > 1, & r = 0, \\ [(1 - R)^2 + F^2]^{1/2}, & r \neq 0. \end{cases} \quad (8)$$

Now we see that the Euler-forward scheme is unconditionally unstable for inertial oscillations if there is no friction ($r = 0$). However, with $r \neq 0$, the model solution might be stable if dissipation of the numerical model is large enough to damp out the numerical instability due to improper discretization in the Coriolis terms, if and only if $1 - (1 - F^2)^{1/2} \leq R \leq 1 + (1 - F^2)^{1/2}$ [the solution is obtained by solving the quadratic equation on R : $(1 - R)^2 + F^2 \leq 1$]. If F^2 is much less than unity, the stability condition reduces to $F^2/2 \leq R \leq 2 - F^2/2$. The lowest limit ($R \geq F^2/2$) gives large and effective dissipation. For example, if $f = 10^{-4} \text{ s}^{-1}$ and $\Delta t = 240 \text{ s}$, associated with this friction is the e -folding timescale $T \sim r^{-1} \text{ s} \sim 9.6 \text{ days}$. The large viscosity necessary for damping in the finite-difference equations significantly ruins physical processes with timescales longer than 10 days, such as mesoscale eddies with timescales from 2 weeks to months and Rossby waves (Dukowicz and Smith 1994). Thus, a proper numerical scheme must be

TABLE 2. The time-step-dependent growth of the eigenvalue $\lambda^n = [(1 - R)^2 + F^2]^{n/2}$ at the end of a 10-day simulation using the Euler-forward scheme, where $F = f\Delta t$ with $f = 10^{-4} \text{ s}^{-1}$. The values in parentheses are the normalized eigenvalues by their true solutions $(1 - R)^n$, that is, the normalized amplifications.

	True solution	Total time steps (n)				
		86 400	17 280	8640	1728	864
Time step Δt (s)		10	50	100	500	1000
$r = 0$	1	1.044	1.241	1.54	8.65	73.59
$r = 2.5 \times 10^{-7} \text{ s}^{-1}$	0.917	0.958	1.138	1.413	7.934	67.559
		(1.044)	(1.241)	(1.541)	(8.65)	(73.656)
$r = 2.5 \times 10^{-6} \text{ s}^{-1}$	0.421	0.44	0.523	0.649	3.652	31.271
		(1.044)	(1.241)	(1.54)	(8.667)	(74.227)

carefully examined to replace this unstable scheme, as will be discussed shortly.

If $\beta = 0.5$, the scheme becomes Euler centered. Taking the absolute value of (7) leads to

$$|\lambda| = \begin{cases} 1, & r = 0, \\ \frac{[(1 - R - F^2/4)^2 + F^2(1 - R/2)^2]^{1/2}}{1 + (F^2/4)} < 1, & r \neq 0. \end{cases} \quad (9)$$

This Euler-centered scheme accurately simulates inertial waves.

If $\beta = 1$, the scheme becomes the Euler-backward scheme, and the eigenvalue modulus of (7) is

$$|\lambda| = \begin{cases} \frac{1}{(1 + F^2)^{1/2}} < 1, & r = 0, \\ \frac{1 - R}{(1 + F^2)^{1/2}} < 1, & r \neq 0. \end{cases} \quad (10)$$

Therefore, the amplitudes of inertial oscillations always attenuate with time.

From (7), we are able to obtain the solution to ω of the finite-difference equation normalized by the exact (analytical) solution $\omega_E = -f$, through some algebraic operations, as

$$\frac{\omega}{-f} = \frac{1}{F} \arctan \left[\frac{F(1 - \beta R)}{1 - R - \beta(1 - \beta)F^2} \right]. \quad (11)$$

We see that the normalized phase frequency $\omega/-f$ is a function of F (0–10), β (0–1), and R (0 – 2.5×10^{-4} , if $0 \leq r \leq 2.5 \times 10^{-6} \text{ s}^{-1}$ and $\Delta t = 100 \text{ s}$) with the weakest dependence on R .

In summary, the Euler-forward scheme ($\beta = 0$) is unconditionally unstable for the inertial mode: the larger

the time step, the faster the model blows up, as will be discussed in the next section and in Table 2. By contrast, the Euler-backward scheme ($0.5 < \beta \leq 1$) always dampens inertial waves (Kwizak and Robert 1971; Oberhuber 1993): the larger the time step, the faster the inertial oscillations are damped. However, the attenuation of the inertial waves depends on the backward magnitude of β ($0.5 < \beta \leq 1$) chosen because the scheme starts to dampen these waves when $\beta > 0.5$. The Euler-centered scheme ($\beta = 0.5$) is the most accurate.

c. Euler predictor–corrector scheme

In order to extend the time integration scheme of the Euler-forward approach without changing the two-time-step (explicit) algorithms, a predictor step and a corrector step are differenced, respectively, as

$$\begin{aligned} w^{n+1*} &= (1 - R)w^n - iFw^n, \\ w^{n+1} &= (1 - R)w^n - iF[\beta w^{n+1*} + (1 - \beta)w^n], \end{aligned} \quad (12)$$

where the superscript asterisk denotes the predicted value. Substituting the predictor step into the corrector step in (12) leads to

$$w^{n+1} = [(1 - R) - F^2\beta - iF(1 - R)\beta - iF(1 - \beta)]w^n, \quad (13)$$

where $0 \leq \beta \leq 1$. To conduct the stability analysis, first, substituting (6) into (13) gives the following eigenvalue equation:

$$\lambda = (1 - R - \beta F^2) - iF(1 - \beta R), \quad (14)$$

and then, taking the absolute value gives

$$|\lambda| = [(1 - R - \beta F^2)^2 + F^2(1 - \beta R)^2]^{1/2}. \quad (15)$$

If $r = 0$ we have

$$|\lambda| = \begin{cases} (1 + F^2)^{1/2} > 1, & \beta = 0, \\ \left(1 + \frac{F^4}{4}\right)^{1/2} > 1, & \beta = \frac{1}{2}, \\ [1 - (2\beta - 1)F^2 + \beta^2 F^4]^{1/2} = 1, & \beta = \frac{1}{2} + \varepsilon \wedge F \leq 1, \\ (1 - F^2 + F^4)^{1/2} < 1, & \beta = 1 \wedge F \leq 1, \end{cases} \quad (16)$$

where ε is a small positive number. The scheme with $\beta = 0$ is unconditionally unstable, with the modulus being proportional to $1 + F^2/2$, exactly the same as the Euler forward scheme. The scheme with $\beta = 1$ slightly damps out the inertial mode if $F < 1$, and the amplification factor retains unity (i.e., neutral) if $F = 1$. Note that when $F > 1$, this predictor–corrector scheme becomes an unstable scheme.

If $\beta = 0.5$, the scheme is still weakly unstable (Mesinger and Arakawa 1976; O'Brien 1986), even though accuracy has been raised one order higher than the Euler-forward scheme. To ensure that the eigenvalues fall

inside the unit circle (Wang 1996), we obtain $\varepsilon = F^2/8 + O(F^4/16)$ by solving the quadratic equation $1 - (2\beta - 1)F^2 - \beta^2 F^4 = 1$ on ε in the third equation of (16), where $\beta = 0.5 + \varepsilon$. For instance, if $f = 10^{-4} \text{ s}^{-1}$, $\Delta t = 10^3 \text{ s}$, then $\varepsilon = 0.0012$. Thus, $\beta = 0.5 + \varepsilon (= 0.50012$ in this example) ensures this scheme to be conditionally ($F \leq 1$) neutral for inertial oscillations. Using this idea, we are able to modify the Euler-forward scheme in a model (Blumberg 1991) to be a neutral scheme with the necessary conditions for stability being $F \leq 1$ and $\beta = 0.5 + F^2/8 + O(F^4/16)$ (Wang and Ikeda 1996).

If $r \neq 0$, (15) becomes

$$|\lambda| = \begin{cases} \sqrt{(1-R)^2 + F^2}, & \beta = 0, \\ \sqrt{(1-R)^2 + \frac{F^4}{4}(1+R^2)}, & \beta = \frac{1}{2}, \\ \sqrt{(1-R)^2 - (1-R)F^2 + F^4} < 1, & \beta = 1 \wedge F \leq 1, \end{cases} \quad (17)$$

From (14), we can obtain the following solution to ω through some algebraic operations:

$$\frac{\omega}{-f} = \frac{1}{F} \arctan \left[\frac{F(1-\beta R)}{1-R-\beta F^2} \right]. \quad (18)$$

We will discuss the solution against F and β in section 2f.

d. Leapfrog (centered) scheme

To complete the investigation, we include the leapfrog (three time step) time integration scheme that is the most widely used scheme in many atmospheric and oceanic models, such as in MICOM (Bleck et al. 1992), POM (Mellor 1991), SPEM (Haidvogel et al. 1991), and many others. Equation (2) can be discretized using the leapfrog time scheme,

$$w^{n+1} = (1 - 2R)w^{n-1} - i2Fw^n. \quad (19)$$

Using the same method, substituting (6) into (19) gives the following second-order equation on λ :

$$\lambda^2 + i2F\lambda - (1 - 2R) = 0. \quad (20)$$

The solutions are

$$\lambda_{1,2} = -iF \pm (1 - 2R - F^2)^{1/2}. \quad (21)$$

Taking the absolute value directly leads to

$$|\lambda_{1,2}| = \begin{cases} 1, & r = 0, \\ (1 - 2R)^{1/2} < 1, & r \neq 0. \end{cases} \quad (22)$$

Thus, the leapfrog scheme can accurately simulate inertial waves in the ocean. For cases of $r \neq 0$, the leapfrog scheme still produces the exact amplitude of inertial

waves as the true solution: $(1 - 2R)^{1/2}$. It is well-known that the negative second mode corresponds to the computational mode and is usually removed by using a time filter (Asselin 1972).

The solution to phase frequency is obtained theoretically from (19) through some algebraic operations as follows:

$$\frac{\omega}{-f} = \frac{1}{F} \arcsin \left(\frac{F}{1-R} \right). \quad (23)$$

e. GFDL (Cox–Bryan or MOM) scheme

Finally, we discuss the numerical scheme used by the GFDL model (Bryan 1969; Cox 1984). Equation (2) can be discretized using the averaged velocity values, between times $n + 1$ and $n - 1$, in the Coriolis terms,

$$w^{n+1} = (1 - 2R)w^{n-1} - i2F[\beta w^{n+1} + (1 - \beta)w^{n-1}]. \quad (24)$$

We observe that the scheme with $\beta = 0, 0.5, 1$ [i.e., the parameter α in the GFDL model, see Cox (1984)] corresponds to the Euler-forward scheme, the Euler-centered scheme, and the Euler-backward scheme, respectively. Substituting (6) into (24), using the same method as before, gives the following second-order equation on λ :

$$\lambda^2 = \frac{[1 - 2R - 4\beta(1 - \beta)F^2] - i2F[1 - \beta + (1 - 2R)\beta]}{1 + 4F^2\beta^2}. \quad (25)$$

Taking the absolute value gives

$$|\lambda_{1,2}| = \pm \left\langle \frac{\{[1 - 2R - 4F^2\beta(1 - \beta)]^2 + 4F^2[1 - \beta + (1 - 2R)\beta]^2\}^{1/2}}{1 + 4F^2\beta^2} \right\rangle. \quad (26)$$

where the negative solution is the computational mode. If $\beta = 0$, the scheme becomes the Euler-forward scheme, reducing (26) to

$$|\lambda_{1,2}| = \begin{cases} (1 + 4F^2)^{1/4} > 1, & r = 0, \\ [(1 - 2R)^2 + 4F^2]^{1/4}, & r \neq 0, \end{cases} \quad (27)$$

which is an unstable scheme.

If $\beta = 0.5$, the scheme becomes the Euler-centered scheme, then (26) becomes

$$|\lambda_{1,2}| = \begin{cases} 1, & r = 0, \\ \frac{[(1 - 2R - F^2)^2 + 4F^2(1 - R)^2]^{1/4}}{(1 + F^2)^{1/2}} < 1, & r \neq 0. \end{cases} \quad (28)$$

This scheme accurately simulates inertial waves if $r = 0$ and slightly dampens the amplitude of inertial waves if $r \neq 0$.

If $\beta = 1$, the scheme becomes the Euler-backward scheme, and the eigenvalue modulus from (26) is

$$|\lambda_{1,2}| = \begin{cases} \frac{1}{(1 + 4F^2)^{1/4}} < 1, & r = 0, \\ \frac{(1 - 2R)^{1/2}}{(1 + 4F^2)^{1/4}} < 1, & r \neq 0. \end{cases} \quad (29)$$

Therefore, the amplitudes of inertial oscillations always attenuate with time and are inversely proportional to F^2 . Thus, the GFDL scheme is able to simulate the inertial motion in the ocean only if $\beta = 0.5$. For cases of $\beta > 0.5$, the scheme starts to dampen the inertial waves. For cases of $0 \leq \beta < 0.5$, the scheme is unstable for the inertial motion.

Similarly, the solution to phase-frequency from (24) is obtained:

$$\frac{\omega}{-f} = \frac{1}{2F} \arctan \left\{ \frac{2F[(1 - \beta) + (1 - 2R)\beta]}{1 - 2R - 4\beta(1 - \beta)F^2} \right\}. \quad (30)$$

f. Phase-frequency errors

Figure 1 shows the normalized phase-frequency errors of the Euler scheme in (11) against F and β for $R = 2.5 \times 10^{-4}$. The results for $R = 2.5 \times 10^{-5}$ (small viscosity) are nearly identical to Fig. 1 and thus are not shown. We see that the phase frequency with $\beta = 0$ (dashed curve, explicit Euler-forward scheme) is iden-

tical to that with $\beta = 1$ (dash-dot curve, Euler-backward scheme), whereas the phase frequency of the Euler-centered scheme has a jump at $F = 1.1$. One common feature is that the phase frequencies of the finite-difference schemes are very close to those of the differential equation when $F \leq 0.1$ only. In other words, the time step Δt in a numerical model can be only taken to be a maximum value of 10^3 s if $f = 10^{-4}$ s $^{-1}$ in order to simulate the correct phase frequency of inertial os-

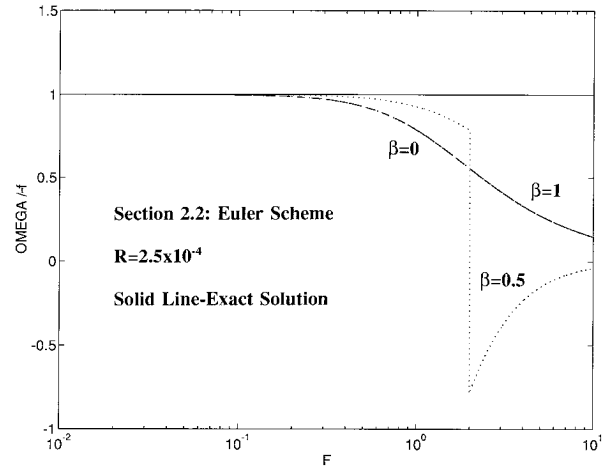


FIG. 1. The normalized phase frequency of the Euler scheme (the ratio of phase frequency of the differencing scheme to that of the exact solution) against F for $\beta = 0$ (dashed curve), 0.5 (dotted), and 1 (dash-dot) for $R = 2.5 \times 10^{-4}$. The values lower (higher) than the solid line ($\omega/-f = 1$) indicate the under- (over-) estimation by the numerical scheme. Note that the negative values indicate the waves rotating cyclonically, in the opposite direction to the true waves rotating anticyclonically. See the discussion in section 2b.

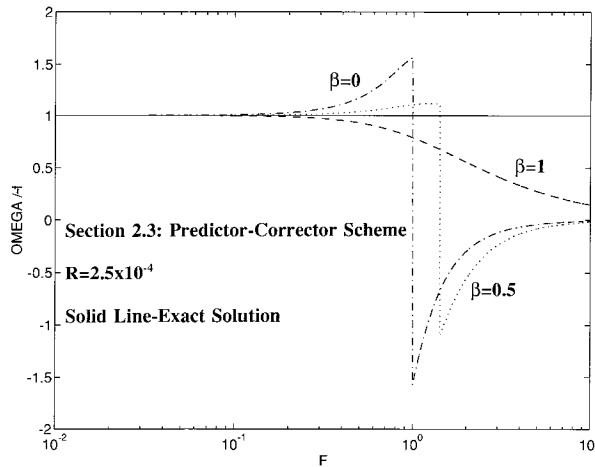


FIG. 2. Same as Fig. 1 except for the Euler predictor-corrector scheme, as discussed in section 2c.

cillations (waves). The smaller the time step, the better the phase information can be preserved. When F is greater than 0.1, the phase frequency of the inertial wave becomes slower (underestimated). When $F \geq 1.1$, the Euler-centered scheme ($\beta = 0.5$, dotted curve with the negative sign) generates a wave rotating cyclonically, that is, in the opposite direction to the analytical solution (anticyclonic oscillation). Overall, when $F < 1$, the Euler-centered scheme preserves the best phase-frequency information.

For the Euler predictor-corrector scheme, the diagram of (18) against F and β is shown in Fig. 2. We see that the Euler-centered scheme ($\beta = 0.5$) preserves the best phase information of inertial oscillation if $F < 1$. The scheme with $\beta = 0$ accelerates (overestimates) the phase frequency and the scheme with $\beta = 1$ slows it down (underestimates). The scheme with $\beta = 0$ has a jump at $F = 1$ where the scheme ($\omega/-f < 0$) generates a wave rotating cyclonically, in the opposite direction to the true wave that rotates anticyclonically. Overall, the phase frequency can be well preserved when $F < 0.1$. When $F \rightarrow \infty$, $\omega/-f \rightarrow 0$, the simulated phase frequency is much slower than the true solution, that is, there are no longer inertial waves in the model.

We now examine the solution of (23) against F for the leapfrog scheme (Fig. 3). The explicit leapfrog scheme accelerates the phase frequency for $0.1 < F < 1.05$. However, the phase frequency information can be preserved very well for $F < 0.1$.

Figure 4 shows $\omega/-f$ [solution of (30)] against F and β (Cox 1984). The forward ($\beta = 0$) and backward ($\beta = 1$) schemes are identical and both, along with the centered scheme ($\beta = 0.5$), underestimate the phase frequency when $F > 0.1$. Nevertheless, the centered scheme improves the solution compared to the other two schemes when $F < 1$. When $F > 1$, the centered scheme produces a wave propagating in the opposite direction to the true solution, whereas the other two still simulate

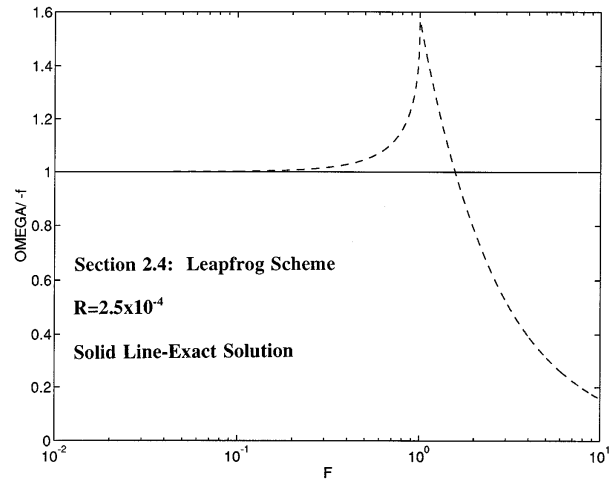


FIG. 3. Same as Fig. 1 except for the leapfrog (centered) scheme, as discussed in section 2d.

the correct direction of the wave, although the phase frequency is underestimated.

3. Comparisons between the numerical and exact solutions

To compare the solutions from finite-difference equations with the differential equations, we set, in both differential and finite-difference equations, $f = 10^{-4} \text{ s}^{-1}$ and $r = 0$ for the nondissipative case and $r = 2.5 \times 10^{-6}$ (10^{-7}) s^{-1} for the dissipative case, which corresponds to the e -folding (decaying) timescale of 4.5 (45) days. The other parameter of concern is the integration time step Δt , which varies from case to case in order to examine the truncation errors that depend on the non-dimensional parameter $F = f\Delta t$.

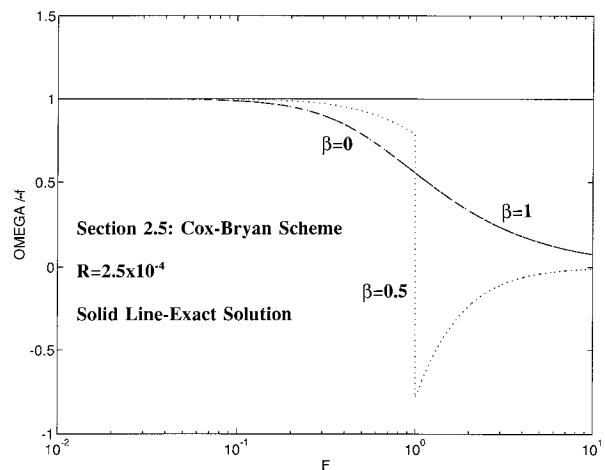


FIG. 4. Same as Fig. 1 except for the GFDL scheme, as discussed in section 2e.

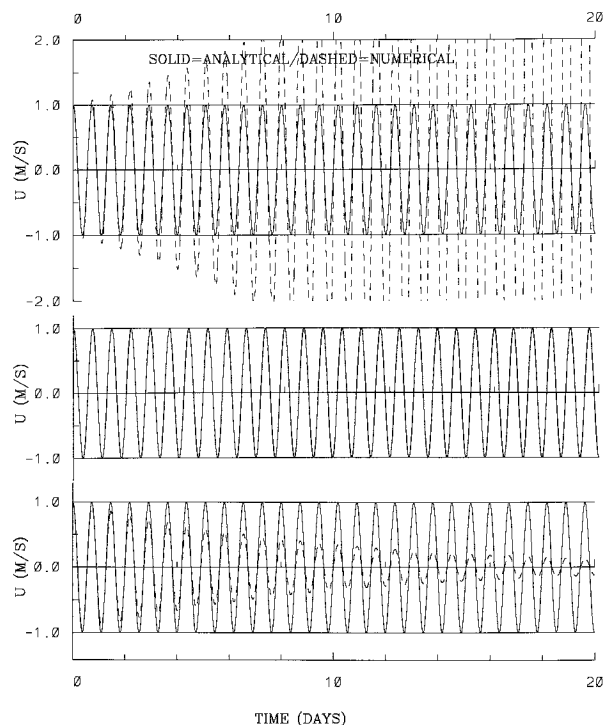


FIG. 5. The time series of inertial current velocity, u only, from analytical (exact) solutions (solid curves) and numerical solutions of the Euler scheme (dashed curves) with $\beta = 0$ (Euler-forward, upper panel), 0.5 (Euler-centered, middle panel), and 1 (Euler-backward, lower panel), as discussed in section 2b. The integration time step is 240 s.

a. Nondissipative case ($r = 0$)

We carried out the following runs using $\Delta t = 240$ s, then $F = f\Delta t = 0.024 < 1$. Figure 5 shows the comparisons between the exact and differential solutions (solid lines) and finite difference or numerical solutions (dashed lines) for $\beta = 0$ (upper panel) as discussed in section 2b, which corresponds to the Euler-forward scheme. The comparisons from the Euler-centered (middle panel) and Euler-backward (lower panel) schemes are also shown, respectively. We clearly see that the Euler-forward scheme ($\beta = 0$) is unconditionally unstable, while the Euler-centered scheme ($\beta = 0.5$) preserves the neutral amplification and the Euler-backward scheme damps out inertial waves.

To emphasize the time-step-dependent growth of the Euler-forward scheme, we conducted a series of 10-day runs using different time steps Δt equal to 10, 50, 100, 500, and 1000 s (see Table 2). It is clear that the larger the time step used in the Euler-forward scheme, the faster the inertial oscillations grow. Even using a time step as short as 10 s, a simulation can be continued only less than 10 days (Table 2).

A consistency between the exact and numerical solutions from the Euler predictor–corrector scheme with $\beta = 0.5$ can be seen (Fig. 6, upper panel) as discussed in section 2c. This scheme can be used to replace the

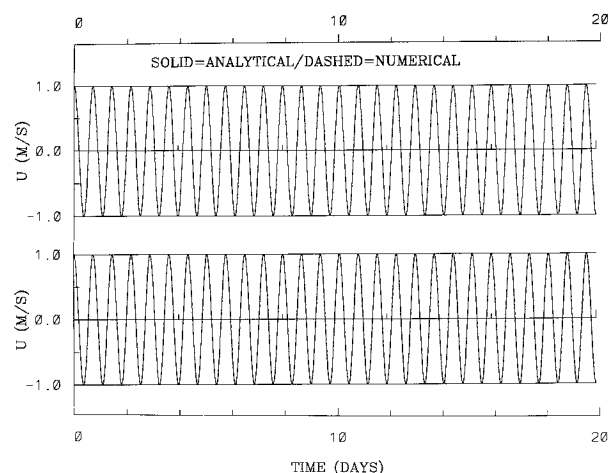


FIG. 6. The time series of inertial current velocity, u only, from analytical (exact) solutions (solid curves) and numerical solutions of the Euler predictor–corrector schemes (dashed curves) with $\beta = 0.5$ in section 2c and of the GFDL scheme with $\beta = 0.5$ (lower panel). The integration time step is 240 s.

Euler-forward scheme. Nevertheless, the scheme with $\beta = 0$ is unconditionally unstable (not shown, see Table 3) and the scheme with $\beta = 1$ corresponds to the dissipative scheme for inertial oscillations (not shown, see Table 3). Figure 6 also shows the comparison of the GFDL scheme for $\beta = 0.5$ only (lower panel), as discussed in section 2e. In accordance with the earlier theoretical analysis, the result with $\beta = 0$ is unconditionally unstable (not shown, see Table 3) because it is equal to the Euler-forward scheme. The centered scheme ($\beta = 0.5$) accurately preserves the amplitude of inertial waves, while the backward scheme ($0.5 < \beta \leq 1$) introduces damping of the inertial motion (not shown, see Table 3) as β increases.

The comparison of the u component only from the leapfrog scheme, as discussed in section 2d, was also conducted (Fig. 7, upper panel). This scheme can well preserve the amplitude of inertial waves.

For an extreme case, we set $\Delta t = 10^4$ s, that is, $F = 1$. Thus, the inertial constraint, $F < 1$, is violated. Figure 8 shows the results from 1) the Euler-centered scheme with $\beta = 0.5$ (see section 2b), 2) the Euler predictor–corrector scheme with $\beta = 0.5$ (see section 2c), 3) the leapfrog scheme (see section 2d), and 4) the GFDL scheme with $\beta = 0.5$ (see section 2e). We see that only the GFDL model is stable, but the phase frequency is incorrectly simulated because of large truncation or round-off errors caused by using the large time step. Thus, the GFDL scheme can well preserve the amplitude of inertial waves for using the large integration time step. This is one of the reasons that this model has been widely used for the long-term simulation of climate change.

Now we further examine the possibility for the long-term integration in the climate study using a large time step violating the inertial constraint, $F \geq 1$. The com-

TABLE 3. A summary of stability analysis and phase frequency errors of different time finite-differencing schemes for inertial oscillations; $F = f\Delta t$ and $R = r\Delta t$.

Numerical scheme	Parameter and its scheme	Modulus of the eigenvalue: $ \lambda $, $r = 0$	Amplitude stability	Normalized phase frequency $\omega/(-f)$
Section 2b: Euler scheme	$\beta = 0$: Euler forward	$(1 + F^2)^{1/2} > 1$	Uncond. unstable	$F^{-1} \arctan$
	$\beta = 0.5$: Euler centered	1	Neutral	$\{F(1 - \beta R)/[1 - R - \beta(1 - \beta)F^2]\}$
	$\beta = 1$: Euler backward	$(1 + F^2)^{1/2} < 1$	Serious damping	
Section 2c: Euler predictor–corrector scheme	$\beta = 0$	$(1 + F^2)^{1/2} > 1$	Uncond. unstable	$F^{-1} \arctan$
	$\beta = 0.5$	$(1 + F^4/4)^{1/2} > 1$	Weakly unstable	$\{F(1 - \beta R)/[1 - R - \beta F^2]\}$
	$\beta = 0.5 + \varepsilon$, $\varepsilon = F^2/8 + O(F^4/16)$	1	Neutral	
	$\beta = 1$	$(1 - F^2 + F^4)^{1/2} < 1$, if $F < 1$	Weak damping	
Section 2d: Leapfrog scheme		1	Neutral	$F^{-1} \arcsin [F/(1 - R)]$
Section 2e: Leapfrog + β -weighted Coriolis terms between $n - 1$ and $n + 1$	$\beta = 0$	$(1 + 4F^2)^{1/2} > 1$	Uncond. unstable	$(2F)^{-1} \arctan$
	$\beta = 0.5$	1	Neutral	$\{2F[(1 - \beta) + \beta(1 - 2R)]/[1 - 2R - 4\beta(1 - \beta)F^2]\}$
	$\beta = 1$	$(1 + 4F^2)^{1/2} < 1$	Serious damping	

parisons using fully implicit schemes ($\beta = 1$) from sections 2b, 2c, and 2e were conducted (Fig. 9). All of the fully implicit schemes ($\beta = 1$) damp out inertial waves very quickly in the first two inertial cycles, except that the predictor–corrector scheme with $\beta = 1$ keeps the same amplitude compared to the exact solution. The simulated phase frequency, however, has large errors, about 180° out of phase to the true solution. Thus, the Euler predictor–corrector scheme with $\beta = 1$ is not suitable for the long-term integration in the climate study. The GFDL (Cox 1984) and the OPYC (Oberhuber 1993) implicit schemes are the best schemes for long-term climate study using a large time step.

b. Dissipative case ($r \neq 0$)

To confirm that the results from the nondissipative case are still valid for the dissipative fluid, we compare

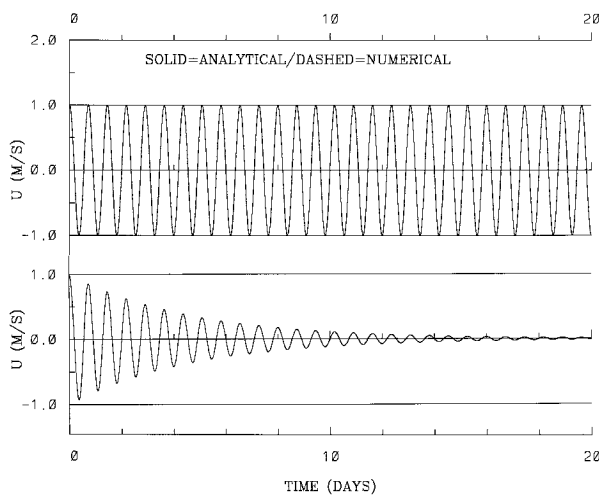


FIG. 7. The time series of inertial current velocity, u only, from analytical (exact) solutions (solid curves) and numerical solutions of the leapfrog scheme (dashed curves) with $r = 0$ (upper panel) in section 2d and with $r = 2.5 \times 10^{-6} \text{ s}^{-1}$ (lower) in section 3b. The integration time step is 240 s.

the results in the dissipative case, which is closer to reality. In the following runs, we set $\Delta t = 240 \text{ s}$ and $r = 2.5 \times 10^{-6} \text{ s}^{-1}$. Note that the viscosity value is large because the corresponding e -folding timescale is only 4.5 days.

Figure 10 shows the exact and numerical solutions for $\beta = 0, 0.5$, and 1 (first to third panels). We see that the result from the Euler-forward scheme (first panel) is still larger than the exact solution (i.e., unstable), unless the large friction coefficient in the finite-difference equations (FDE), $r_{\text{FDE}} = 2r$, has to be used to damp out the inertial instability induced by the incorrect time integration scheme (the fourth panel). Note that r_{FDE} is two times the value r ($r = 2.5 \times 10^{-6} \text{ s}^{-1}$) used in the analytical model.

Figure 11 shows the exact solutions and numerical solutions of the Euler predictor–corrector scheme only for $\beta = 0.5$ (upper panel). The predictor–corrector scheme with $\beta = 0.5$ simulates very well the inertial mode, while the results with $\beta = 0$ and 1 are unstable and decaying with time, respectively (not shown).

The exact and numerical solutions of the leapfrog scheme are compared with the same friction coefficient (lower panel of Fig. 7). The leapfrog scheme for both nondissipative and dissipative cases simulates well the inertial oscillations.

Similarly, comparison between the exact and numerical solutions of the GFDL scheme for $\beta = 0.5$ only, with the same friction coefficient, was also carried out (Fig. 11, lower panel). We see that the GFDL scheme with $\beta = 0.5$ is able to accurately simulate the inertial motion with some damping in the dissipative case, while the scheme with $\beta = 0$ always produces unstable inertial waves (not shown, because it is the same as the scheme in section 2b, except for an increase in amplitude by a factor of 2 due to the leapfrog scheme). The scheme with $\beta = 1$ (fully implicit) always dampens the inertial mode (not shown).

More runs have also been conducted for small vis-

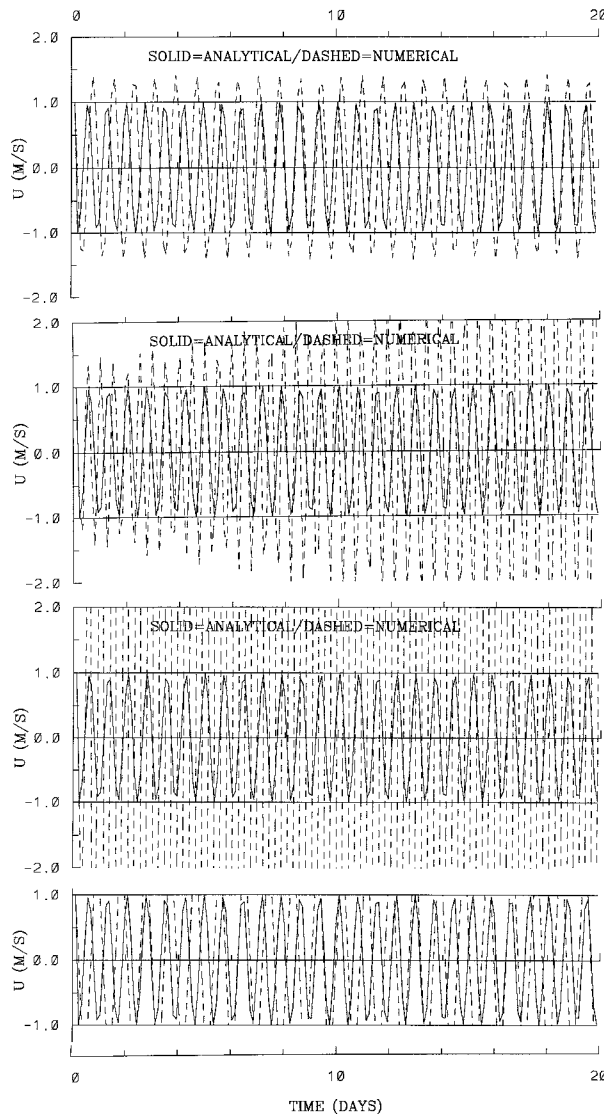


FIG. 8. The time series of inertial current velocity, u only, from analytical (exact) solutions (solid curves) and numerical solutions (dashed curves) of the Euler-centered scheme (upper panel, $\beta = 0.5$ in section 2b), Euler predictor-corrector scheme with $\beta = 0.5$ (second, in section 2c), leapfrog scheme (third, $\beta = 0$ in section 2d), and GFDL scheme with $\beta = 0.5$ (fourth, in section 2e). The integration time step is 10^4 s.

cosity, $r = 2.5 \times 10^{-7} \text{ s}^{-1}$ (e -folding timescale is 45 days). The results are similar to those discussed above, except that the unstable schemes simulate much faster growing inertial waves because of small dissipation (not shown). When $r \rightarrow 0$, the results approach those discussed in section 3a with $r = 0$.

Similar to the nondissipative case, we also conducted the amplification growth of inertial oscillations calculated from the Euler forward scheme using different time steps for both small and large viscosity cases: $r = 2.5 \times 10^{-7} \text{ s}^{-1}$ and $r = 2.5 \times 10^{-6} \text{ s}^{-1}$ (see Table 2). As we see, the normalized amplitudes (amplification)

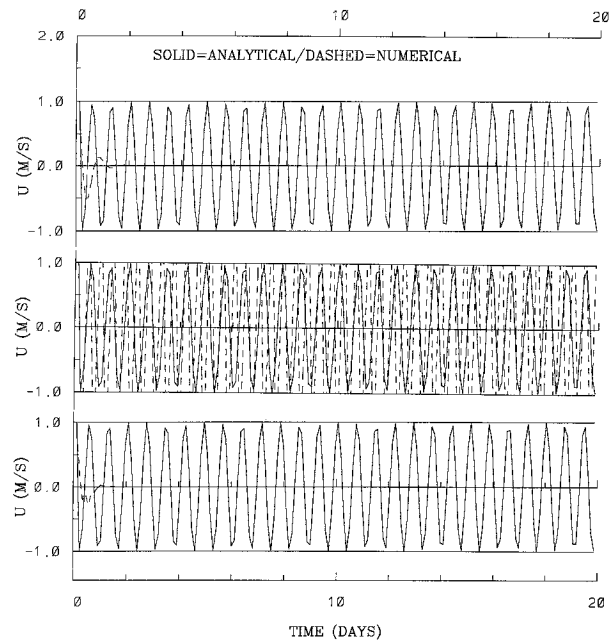


FIG. 9. The time series of inertial current velocity, u only, from analytical (exact) solutions (solid curves) and numerical solutions (dashed curves) of the Euler-backward scheme (upper panel, $\beta = 1$ in section 2b), the Euler predictor-corrector scheme with $\beta = 1$ (second, in section 2c), and the GFDL scheme with $\beta = 1$ (third, in section 2e). The integration time step is 10^4 s.

are the same as those with $r = 0$, independent of viscosity values. In other words, the Euler-forward scheme is still unstable for the inertial mode in the dissipative flow in terms of normalized amplification by its true solution, unless a larger viscosity (at least twice as large as the physical viscosity) has to be used.

4. Conclusions and discussion

Based on the careful investigations in the preceding sections, we can construct Table 3 as our summary.

- 1) To correctly simulate inertial waves and the geostrophic adjustment process in the ocean and coastal seas, four types of time integration schemes are recommended for such an application. They are 1) the Euler-centered ($\beta = 0.5$) scheme for the Coriolis terms with forward differencing in time (Dietrich et al. 1987); 2) the Euler predictor-corrector scheme with $\beta = 0.5 + \varepsilon$ ($\varepsilon = F^2/8$); 3) the leapfrog scheme, such as in MICOM, POM, SPEN, and many others; and 4) the leapfrog scheme with the Euler-centered Coriolis terms ($\beta = 0.5$) only in the GFDL model.
- 2) The Euler-forward scheme with $\beta = 0$ (Blumberg 1991), the Euler predictor-corrector scheme with $\beta = 0$, and the GFDL scheme with $\beta = 0$ (Cox 1984) are inertially unstable schemes and must be avoided by modelers unless the modeled systems are highly dissipative. In other words, the Euler-forward scheme creates serious numerical inertial instability

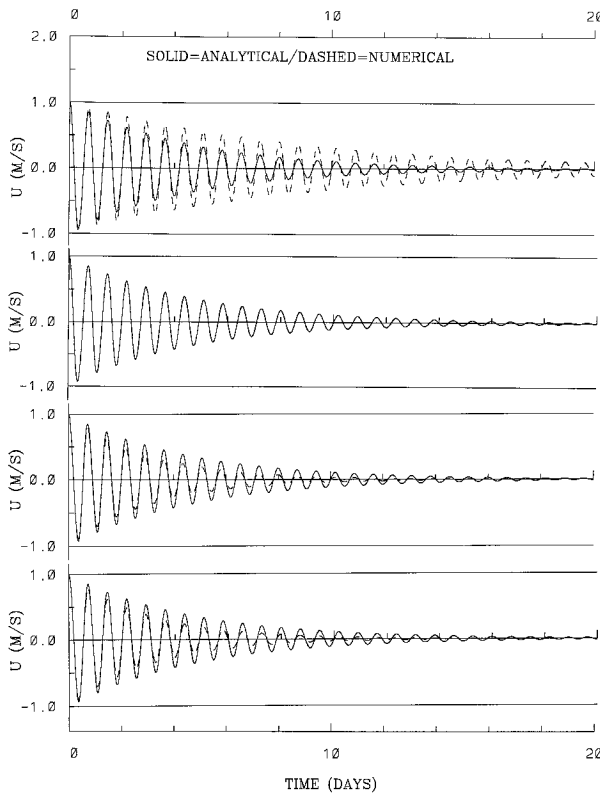


FIG. 10. The time series of inertial current velocity, u only, from analytical (exact) solutions (solid curves) and numerical solutions (dashed curves) with $r = 2.5 \times 10^{-6} \text{ s}^{-1}$ of the Euler-forward scheme ($\beta = 0$, first panel), the Euler-centered scheme ($\beta = 0.5$, second panel), and the Euler-backward scheme ($\beta = 1$, third panel) in section 2b. The fourth panel is the same as the first panel except $r_{\text{FDE}} = 2r$. The integration time step is 240 s.

once it is used without enough large viscosity and diffusivity. We have developed the Euler predictor–corrector scheme with $\beta = 0.5 + (f\Delta t)^2/8$ to replace the Euler-forward scheme without changing the explicit two-time-step approach (Wang and Ikeda 1996).

- 3) For the long-term climate change simulations, the long integration time step violating $F < 1$ in the model is usually used. Thus, the implicit numerical scheme for the Coriolis terms must be used to remove this inertial constraint (i.e., $F < 1$) by damping inertial waves in the first two inertial tidal cycles. Only two schemes, the OPYC scheme in section 2b with $0.5 + (f\Delta t)^2/8 < \beta \leq 1$ (Oberhuber 1993) and the GFDL scheme in section 2e with $0.5 < \beta \leq 1$, can serve this purpose. For example, in the OPYC model, a value of $\beta = 0.75$ is usually applied (J. M. Oberhuber 1996, personal communication). All of the centered treatments of the Coriolis terms ($\beta = 0.5$) discussed in this paper cannot be used for the long-term model integration using a large time step violating $F < 1$.
- 4) To correctly simulate the phase frequency of the in-

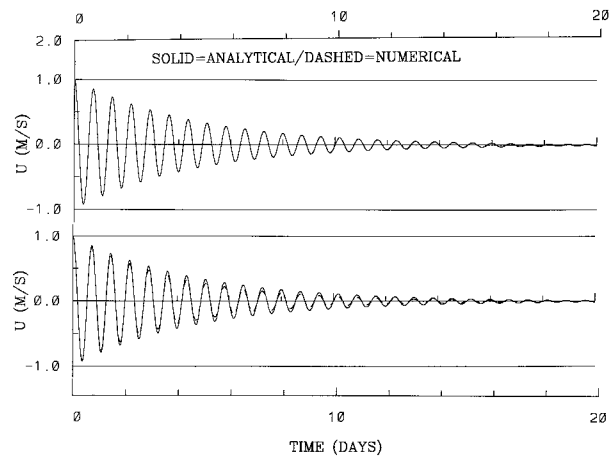


FIG. 11. The time series of inertial current velocity, u only, from analytical (exact) solutions (solid curves) and numerical solutions (dashed curves) of the Euler predictor–corrector scheme with $\beta = 0.5$ (upper panel) in section 2c and of the GFDL scheme with $\beta = 0.5$ (lower panel) in section 2e for $r = 2.5 \times 10^{-6} \text{ s}^{-1}$. The integration time step is 240 s.

ertial wave, $F < 0.1$ is strongly recommended. Generally speaking, the explicit leapfrog and predictor–corrector schemes ($0 \leq \beta \leq 0.5$) overestimate the phase frequency, while the Euler schemes ($0 \leq \beta \leq 1$) and implicit schemes ($0.5 < \beta \leq 1$) underestimate it. The Euler-centered schemes are the most accurate when $F < 1$. When F becomes large, the simulated phase frequency is much slower than the true solution, that is, $\omega/-f \rightarrow 0$ (no inertial waves). Thus, the alternate use of an explicit scheme and (periodic use of) an implicit scheme will cancel out the phase error (speeding or slowing down) produced by using a single (explicit or implicit) scheme only, and vice versa. For example, in the GFDL model, SPeM, and other coastal ocean models, a leapfrog scheme is used together with a periodic (e.g., every 10 time steps) use of an Euler-backward scheme in order to correct the overestimated phase frequency induced by the explicit leapfrog scheme.

Finally, it should be pointed out that quite a few coastal ocean models in oceanographic literature still use an explicit Euler-forward scheme that has been proven to be an unstable scheme. This scheme can be stable only if the model horizontal or vertical eddy viscosity (or numerical viscosity produced by the semi-implicit or implicit schemes for advection) is at least two times larger than the physical viscosity to dampen the (numerical) inertial instability. This kind of model cannot be used for a long simulation with the timescale of the physical processes longer than 10 days and seriously ruins other physical processes, even the tidal (surface) gravity waves. An easy, economic way to amend those models using Euler-forward scheme is to replace the Euler-forward scheme with the Euler predictor–corrector scheme as proposed in section 2c (Wang and Ikeda

1996) without changing its original two-time-step algorithm (i.e., with little programming). However, as a penalty, the Euler predictor–corrector scheme is more expensive than the leapfrog scheme.

Acknowledgments. We thank C. Hannah, K.-T. Tee, and A. van der Baaren of BIO for their constructive comments on a draft of this paper. J. Wang acknowledges the support mainly from the NSERC of Canada through a Government Lab Postdoctoral Fellowship held at the Bedford Institute of Oceanography (90%), partly from EVOS Trusteeship Council via the Prince William Sound Science Center (Cordova, Alaska) (5%), and partly from USCG and NOAA for the South Florida Oil Spill Research Center, to the University of Miami (5%). The authors thank one anonymous reviewer and Dr. J. Oberhuber for their very constructive comments that helped improve the presentation by clarifying some terminology and listing numerical schemes some ocean models use (Table 1).

REFERENCES

- Asselin, R., 1972: Frequency filter for time integrations. *Mon. Wea. Rev.*, **100**, 487–490.
- Becker, J.-M., and E. Deleersnijder, 1993: Stability of a FBTCS scheme applied to the propagation of shallow water inertia-gravity waves on various space grids. *J. Comput. Phys.*, **108**, 95–104.
- Bleck, R., C. Rooth, D. Hu, and L. Smith, 1992: Salinity-driven thermocline transients in a wind- and thermohaline-forced isopycnal coordinate model of the North Atlantic. *J. Phys. Oceanogr.*, **22**, 1486–1505.
- Blumberg, A. F., 1991: A primer for ECOM-si. Tech. Rep. for HydroQual, Inc., 66 pp.
- Bryan, K., 1969: A numerical method for the study of the circulation of world ocean. *J. Comput. Phys.*, **4**, 347–376.
- Cox, M. D., 1984: A primitive equation, three-dimensional model of the ocean. GFDL Ocean Group Tech. Rep. 1.
- Dietrich, D. E., M. G. Marieta, and P. J. Roache, 1987: An ocean modeling system with turbulent boundary layers and topography: Numerical description. *Int. J. Num. Methods Fluids*, **7**, 833–855.
- Dukowicz, J. K., and R. D. Smith, 1994: Implicit free-surface method for the Bryan–Cox–Semtner ocean model. *J. Geophys. Res.*, **99**, 7991–8014.
- Grotjahn, R., and J. J. O'Brien, 1976: Some inaccuracies in finite differencing hyperbolic equations. *Mon. Wea. Rev.*, **104**, 180–194.
- Haidvogel, D., J. Wilkin, and R. Young, 1991: A semi-spectral primitive equation ocean circulation model using vertical sigma and orthogonal curvilinear horizontal coordinates. *J. Comput. Phys.*, **94**, 151–185.
- Kunze, E., and T. B. Sanford, 1984: Observations of near-inertial waves in a front. *J. Phys. Oceanogr.*, **14**, 566–581.
- Kwizak, M., and A. J. Robert, 1971: A semi-implicit scheme for grid point atmospheric models of primitive equations. *Mon. Wea. Rev.*, **99**, 32–36.
- Maas, L. R. M., and J. J. M. van Haren, 1987: Observations on the vertical structure of tidal and inertial currents in central North Sea. *J. Mar. Res.*, **45**, 293–318.
- Mellor, G. L., 1991: Users guide for a three-dimensional, primitive equation, numerical model. Atmospheric and Oceanic Sciences Program, 39 pp.
- Mesinger, F., and A. Arakawa, 1976: Numerical methods used in atmospheric models. GARP Pub. Series 17, Vol. 1.
- Millot, C., and M. Crepon, 1981: Inertial oscillations on the continental shelf of the Gulf of Lion—Observations and theory. *J. Phys. Oceanogr.*, **11**, 639–657.
- Oberhuber, J. M., 1993: Simulation of the Atlantic circulation with a coupled sea ice-mixed layer-isopycnal general circulation model. Part I: Model description. *J. Phys. Oceanogr.*, **23**, 808–829.
- O'Brien, J. J., 1986: Time integration schemes. *Advanced Physical Oceanographic Numerical Modeling*, J. J. O'Brien, Ed., NATO ASI Series, Reidel, 155–164.
- Pollard, R. T., and R. C. Millar Jr., 1970: Comparison between observed and simulated wind-generated inertial oscillations. *Deep-Sea Res.*, **17**, 813–821.
- Robert, A., J. Henderson, and C. Turnbull, 1972: An implicit time integration scheme for baroclinic models of the atmosphere. *Mon. Wea. Rev.*, **100**, 329–335.
- Schott, F., 1970: Spatial structure of inertial-period motions in a two-layered sea, based on observations. *J. Mar. Res.*, **29**, 85–102.
- Tee, K.-T., 1979: The structure of three-dimensional tide-generating currents. Part I: Oscillating current. *J. Phys. Oceanogr.*, **9**, 930–944.
- Wang, J., 1996: Global linear stability of the 2-D shallow-water equations: An application of the distributive theorem of roots for polynomials in the unit circle. *Mon. Wea. Rev.*, **124**, 1301–1310.
- , and M. Ikeda, 1996: A 3-D ocean general circulation model for mesoscale eddies—I: Meander simulation and linear growth rate. *Acta Oceanol. Sin.*, **15**, 31–58.
- , R. G. Ingram, and L. A. Mysak, 1991: Variability of internal tides in the Laurentian Channel. *J. Geophys. Res.*, **96**, 16 859–16 875.